



Original article

Sulfonamides containing coumarin moieties selectively and potently inhibit carbonic anhydrases II and IX: Design, synthesis, inhibitory activity and 3D-QSAR analysis



Zhong-Chang Wang¹, Ya-Juan Qin¹, Peng-Fei Wang¹, Yong-An Yang, Qing Wen, Xin Zhang, Han-Yue Qiu, Yong-Tao Duan, Yan-Ting Wang, Ya-Li Sang, Hai-Liang Zhu*

State Key Laboratory of Pharmaceutical Biotechnology, Nanjing University, Nanjing 210093, People's Republic of China

ARTICLE INFO

Article history:

Received 8 February 2013

Received in revised form

13 April 2013

Accepted 15 April 2013

Available online 9 May 2013

Keywords:

Sulfonamide derivatives

Carbonic anhydrase

Antitumor activity

3D-QSAR

CCK-8 assay

ABSTRACT

A series of sulfonamides containing coumarin moieties had been prepared that showed a very interesting profile for the inhibition of two human carbonic anhydrase inhibitors. These compounds were evaluated for their ability to inhibit the enzymatic activity of the physiologically dominant isozymes hCA II and the tumor-associated isozyme hCA IX. The most potent inhibitor against hCA II and IX were compounds **5d** (IC₅₀ = 23 nM) and **5l** (IC₅₀ = 24 nM), respectively. These sulfonamides containing coumarin moieties may prove interesting lead candidates to target tumor-associated CA isozymes, wherein the CA domain is located extracellularly. Eighteen compounds were scrutinized by CoMFA and CoMSIA techniques of 3D quantitative structure–activity relationship. Nine of the compounds were evaluated for cytotoxicity against human macrophage.

© 2013 Elsevier Masson SAS. All rights reserved.

1. Introduction

The carbonic anhydrases (CAs, EC 4.2.1.1) are ubiquitous zinc enzymes which are involved in pH buffering of extra- and intracellular spaces by catalyzing the reversible hydration of carbon dioxide and water to bicarbonate and a proton: $\text{CO}_2 + \text{H}_2\text{O} \leftrightarrow \text{HCO}_3^- + \text{H}^+$ [1]. This reaction is known to regulate a broad range of physiological functions which has proven a reliable treatment for a range of human disease states by the respiration and transport of $\text{CO}_2/\text{HCO}_3^-$ [2]. Carbonic anhydrases, specifically isozymes IX (CA IX) is the most strongly overexpressed gene in response to hypoxia in human cancer cells including breast, clear cell renal, colorectal, head and neck, and nonsmall cell lung carcinomas [3]. This enzyme is a multidomain protein with the CA subdomain situated outside the cell and possessing a very high CO_2 hydrase catalytic activity, which is also inhibited by the classical CA inhibitors belonging to the sulfonamide, sulfamate, and sulfamide classes of compounds [4]. There are evidences that CA IX contributes to creating a pH-regulating system suitable for cell viability

and proliferation which make for the extracellular acidification of the solid tumor microenvironment. Tumor cells are prone to survive in hypoxic and acidic microenvironment owing to these enzymes [5]. Hypoxic tumor cells alter their metabolism that favors cell survival and migration, when in a hypoxic conditions to survive, proliferate, and metastasize [6]. Hypoxia-inducible factor (HIF), in addition to genetic and epigenetic changes, is largely responsible for alterations in cell metabolism in hypoxic tumor cells—one core aspect of which is the shift from aerobic to fermentative glycolysis [7]. Fermentative glycolysis leads to elevated lactic acid production; hence, a drop in the intracellular pH (pH_i) of hypoxic tumor cells is expected unless pH homeostasis is established [8]. Suggested by Svastova et al., the assumption that pH_e in different tumor cell cultures recovers to an extent more normal range along with a remarkable increased apoptosis of the tumor cells, when CA IX is inhibited by potent and selective sulfonamide inhibitors is being widely accepted [9]. For example, Pouyssegur's group showed recently that in hypoxic LS174Tr tumor cells expressing either one or both CA isoforms, in response to a “CO₂ load”, both enzymes contribute to extracellular acidification and to maintain a more alkaline resting intracellular pH (pH_i), an action that preserves ATP levels and cell survival in a range of acidic outside pH (6.0–6.8) and low bicarbonate medium. *In vivo* experiments showed that silencing of CA IX alone leads to a 40%

* Corresponding author. Tel./fax: +86 25 83592672.

E-mail address: zhuhl@nju.edu.cn (H.-L. Zhu).

¹ These three authors equally contributed to this paper.

reduction in xenograft tumor volume, with up-regulation of the second gene, that encoding for CA XII, whereas invalidation of both CA IX and CA XII gives an impressive 85% reduction of tumor growth [10]. Accompany with the fact that it has been shown earlier that some CA inhibitors do demonstrate potential antitumor activity *in vivo* [11], CA IX inhibition may compose a fascinating new approach for the management of hypoxic tumors, which generally do not respond to the classical radio- and chemotherapy [12].

One approach aimed at improving the selectivity of tumor cell killing by antitumor drugs mainly using prodrugs with less toxicity which target the tumor cells by special physiology of tumor cells such as selective enzyme expression or hypoxia and therefore are highly specific active to tumor cells [13]. To characterize the potential effect of inhibition of CA IX and XII in tumor hypoxia, there is an implied need to develop small molecules, which are capable of targeting tumor cells to make for experimental advances [14]. Since the discovery of E-7010 in 1992 [15], sulfonamides have emerged as an important class of anticancer agents which interact with a wide range of different cellular targets. Such that indisulam (E7070 [16], HMN-214 [17], T138067 [18]) is in phase II clinical trials as an antitumor sulfonamide with a complex mechanism of action also involving CA inhibition of several isozymes participating in tumor genesis (Fig. 1).

Sulfonamides constitute an important class of drugs, and they possess various types of biological properties including anti-carbonic anhydrase [19], antibacterial [20]. Many of structurally novel sulfonamide derivatives have recently been reported to show substantial antitumor activity, both *in vitro* and *in vivo*. Some of these derivatives are currently being evaluated in clinical trials. Optimistically, these may lead to novel alternative anticancer drugs, devoid of the side effects of the presently available pharmacological agents [21].

Moreover, Claudiu T. Supuran's group reported a novel class of inhibitors of the metalloenzyme carbonic anhydrase with coumarins [22]. All these findings encouraged us to explore the synthesis of sulfonamides containing coumarin moieties and evaluate their activities as antitumor agents.

In this paper we report the synthesis of a series of sulfonamides containing coumarin moieties CAIs that possess high affinity for CA IX, an acceptable selectivity profile for inhibiting the tumor-associated isoforms CAs IX over the cytosolic ones CAs II, and excellent *in vivo* inhibitory effects in a breast cancer xenograft model.

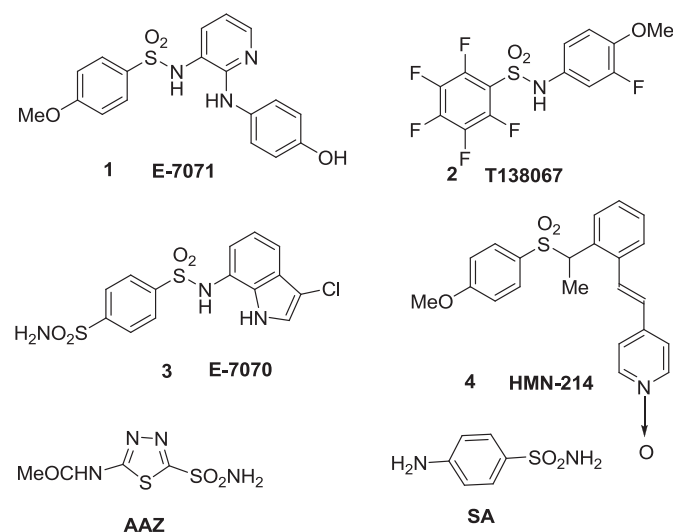


Fig. 1. Known human CA inhibitors including some clinically used drugs.

2. Results and discussion

According to the analysis of the CA active site and the structure of inhibitors [23], Thiry et al. [24] ever reported a general pharmacophore (Fig. 2) for the compounds which acted as carbonic anhydrase inhibitors. In order to make the pharmacophore interact with CA inhibitors, it should include the structural elements that are required to be present in the compounds. This pharmacophore matches this requirement well. A sulfonamide moiety should be included which coordinates with the zinc ion of the active site of the CA and the sulfonamide is attached to a scaffold which is usually a benzene ring. The side chain, which might interact with the hydrophobic and hydrophilic parts of the CA active site, can substitute an aromatic or heterocyclic sulfonamide scaffold. Therefore, different hydrophobic side chains were incorporated in the sulfonamide scaffold with an amide linker that can interact with the hydrophilic part of the active site, and a hydrophobic moiety which can interact with the hydrophobic part of the CA active site.

Fig. 3 illustrates representative examples of the newly synthesized compounds showing compliance with the above-mentioned pharmacophore model and the compounds which were synthesized according to Scheme 1.

2.1. Chemistry

All novel sulfonamides containing coumarin moieties carbonic anhydrase IX inhibitors (5a–5j) described herein were synthesized following the synthetic pathway depicted in Scheme 1. The starting diverse substituted malonic acid mono phenol esters were synthesized by Meldrum's acid and different substituted phenol under a solvent-free condition in high yield, then cyclized by Eaton's reagent (phosphoric anhydride and methylsulfonic acid) in mild conditions to give corresponding 4-hydroxycoumarin 3a–3c [25]. The different substituted 3-formyl-4-chlorocoumarin 4a–4c were synthesized by a Vilsmeier–Haack reactions. Subsequently, compounds 5a–5r were prepared from reaction of 4a–4c with the corresponding different substituted sulfonamide in ethanol at room temperature. The reactions were monitored by thin layer chromatography (TLC) and the crude products were purified by recrystallization with ethanol, ethyl acetate and acetone (1:1:0.05). The chemical structures of these sulfonamides containing coumarin moieties were summarized in Table 1. All of the target compounds gave satisfactory analytical and spectroscopic data, which in accordance with their depicted structures by ^1H NMR, ESI MS.

2.2. Biological activity

2.2.1. Antitumor assay and CCK-8 assays

In the present work, eighteen of the newly synthesized compounds 5a–5r were evaluated on their *in vitro* growth inhibitory

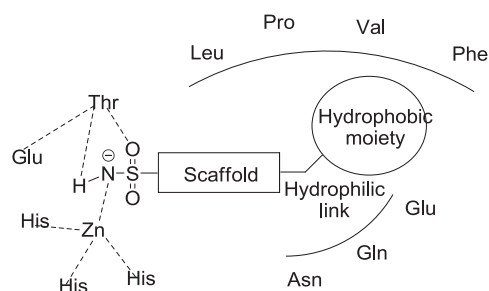


Fig. 2. Structural elements of CA inhibitors in the CA enzymatic active site.

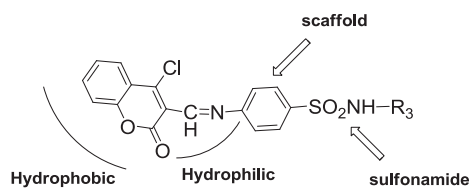


Fig. 3. Representative examples of the synthesized compounds showing compliance to the general pharmacophore of sulfonamide compounds acting as carbonic anhydrase inhibitors.

activities against two cultured cell lines, which are mouse melanoma cells (B16-F10) and breast carcinoma cell lines (MCF-7) in comparison to the known anticancer drugs: doxorubicin and semaxanib as reference drugs. IC_{50} values were calculated using an inhibitory model, with the sum of squares of the residuals minimized by Origin 8.6 software. The values obtained for the eighteen compounds against the B16-F10 and MCF-7 cell lines were shown in Table 1. As shown in Table 1, it was observed that sulfonamides containing coumarin moieties had been found to show the inhibition of growth of two tumor cell lines with moderate IC_{50} values. For MCF-7 cell line which over-expressed CA that previously references had reported, sulfonamide derivatives in particular displayed more potent anti-tumor activity than the other one tumor cell lines. The IC_{50} values of most sulfonamides containing coumarin moieties ranged from 0.0088 μ M to 0.16 μ M in MCF-7. Among them, compound **5j** displayed the most potent anti-tumor activity with IC_{50} of 0.0088 μ M, compared to the positive control doxorubicin (IC_{50} = 0.072 μ M) and semaxanib (IC_{50} = 0.012 μ M). Nevertheless, IC_{50} values would have a 1–10 folds in B16-F10 on average. More potent anti-tumor activity for MCF-7 together with virtual screening results both indicated that the over-expressed CA might be a potential target which these sulfonamides containing coumarin moieties interacted with.

2.2.2. Carbonic anhydrase inhibition

Inhibition of two physiologically relevant CA isoforms with compounds **5a–5r**, AAZ and SA, two clinically used drugs were presented in Table 1 [26]. HCA II (cytosolic, widespread enzymes) and IX (transmembrane, tumor-associated CAs) have been included in this study because of their relevance as targets/off targets when developing CAIs [27].

CA IX is highly expressed in breast malignancies, and studies have demonstrated that CA IX and CA XII are variably expressed in breast cancer cell lines. Furthermore, CA IX is associated with a poor

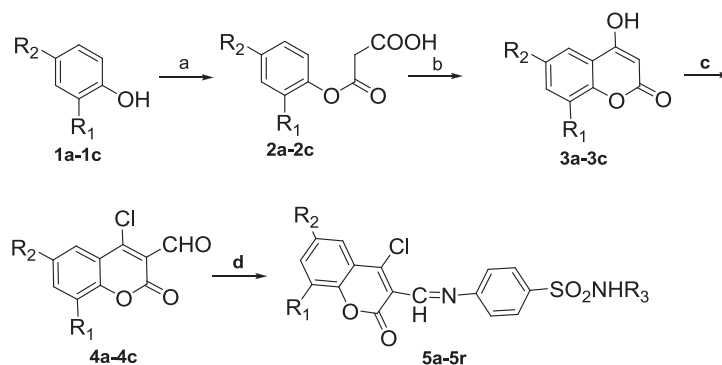
prognosis for patients with breast cancer and it is significantly associated with distant metastasis (Lou et al., unpublished results). Therefore, we have chosen breast cancer as a malignancy model in which to test, *in vivo*, the inhibitory activity of some of the CA IX inhibitors described here [10]. So, the newly described sulfonamides containing coumarin moieties **5a–5r** were tested in an *in vitro* carbonic anhydrase assay to evaluate their potential as antitumor drugs. The results are summarized in Table 1 as IC_{50} values.

The following structure–activity relationship (SAR) can be observed from data of Table 1, CA activities of these compounds were tested against the standard clinically used inhibitors AAZ and SA. The physiologically dominant and highly active cytosolic isoform hCA II was inhibited by compounds **5a–5r** with IC_{50} in the range of 0.023–0.217 μ M. Compound **5d** was the most active having IC_{50} value of 0.023 μ M, whereas compound **5q** was the least active with IC_{50} value of 0.217 μ M. We simplified the situations by only treating steric complexities as the single factor to deal with. Most of these compounds with un-substituted moieties on the benzene ring of the coumarin and the same substituted moieties on the amino were more effective as hCA II inhibitors compared to those with substituted moieties on the benzene ring of the coumarin, for instance the active gradient is $-H > -CH_3 > -tBu$. But for hCA IX it's $-CH_3 > -tBu > -H$. Moreover, the tumor-associated isoform hCA IX was inhibited by compounds **5a–5r** with IC_{50} in the range of 0.024–0.188 μ M (Table 1). Result indicated that the sulfonamides incorporating the coumarin moiety lead to highly effective hCA IX inhibitors. In the series of reported compounds with the same substituted moieties on the coumarin, the best inhibitors were incorporating methylpyrimidine. Compound **5l** was the most active having IC_{50} value of 0.024 μ M, whereas compound **5c** was the least active with IC_{50} value of 0.188 μ M. From above, we can conclude compounds **5d** and **5l** had been identified as the most potent inhibitors.

2.2.3. Cytotoxicity

Nine compounds selected on the basis of their structural features were evaluated for their toxicity against human macrophage with the median cytotoxic concentration (CC_{50}) data of tested compounds by the CCK-8 assay, as showed in Table 2. These compounds were tested at multiple doses to study the viability of macrophage.

As shown in Table 2, nine compounds showed that they almost did not exhibit cytotoxic activity. So, we guess that all other compounds were not exhibit cytotoxic activity *in vitro* against macrophage.



^a Reagents and conditions: (a) Meldrum's acid, 2–4 h, 90.6–93.7%; (b) Eaton's reagent, 1–4 h, 78.7–90.9%; (c) DMF/ $POCl_3$, 3 h, 58.6–72.8%; (d) 1.0 equiv p - R_3 NHSO₂PhNH₂, CH₃CH₂OH, 50 °C, 8 h, 44.8–87.9%;

Scheme 1.

Table 1
Anticancer activities (IC₅₀, μM) of sulfonamides containing coumarin moieties (**5a–5r**).

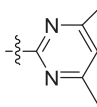
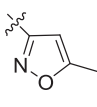
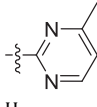
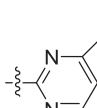
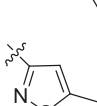
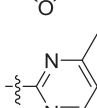
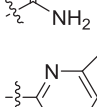
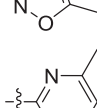
Compounds	R ₁	R ₂	R ₃	IC ₅₀ (μM) ^a	IC ₅₀ (μM) ^a	IC ₅₀ (μM) ^c	IC ₅₀ (μM) ^c
				B16-F10 ^b	MCF-7 ^b	hCAs II ^d	hCA IX ^d
5a	H	H		0.30	0.12	0.033	0.091
5b	H	H		0.30	0.16	0.058	0.138
5c	H	H		0.18	0.058	0.085	0.188
5d	H	H		0.17	0.020	0.023	0.124
5e	H	H		0.27	0.012	0.026	0.141
5f	H	H		0.23	0.031	0.051	0.084
5g	CH(CH ₃) ₃	CH(CH ₃) ₃	H	0.24	0.016	0.112	0.034
5h	CH(CH ₃) ₃	CH(CH ₃) ₃		0.16	0.012	0.122	0.051
5i	CH(CH ₃) ₃	CH(CH ₃) ₃		0.25	0.018	0.103	0.074
5j	CH(CH ₃) ₃	CH(CH ₃) ₃		0.22	0.0088	0.173	0.090
5k	CH(CH ₃) ₃	CH(CH ₃) ₃		0.24	0.064	0.173	0.043
5l	CH(CH ₃) ₃	CH(CH ₃) ₃		0.19	0.032	0.063	0.024
5m	H	CH ₃	H	0.36	0.27	0.088	0.085
5n	H	CH ₃		0.28	0.033	0.121	0.087
5o	H	CH ₃		0.24	0.067	0.100	0.050
5p	H	CH ₃		0.30	0.025	0.141	0.067
5q	H	CH ₃		0.25	0.016	0.217	0.052
5r	H	CH ₃		0.27	0.061	0.061	0.048
Doxorubicin	–	–	–	0.072	0.065	–	–
Semaxanib	–	–	–	0.0036	0.0031	–	–

Table 1 (continued)

Compounds	R ₁	R ₂	R ₃	IC ₅₀ (μM) ^a	IC ₅₀ (μM) ^a	IC ₅₀ (μM) ^c	IC ₅₀ (μM) ^c
				B16-F10 ^b	MCF-7 ^b	hCAs II ^d	hCA IX ^d
AAZ	–	–	–	–	–	0.016	0.028
SA	–	–	–	–	–	0.26	0.29

^a Antiproliferation activity was measured using the CCK-8 assay. Values are the average of three independent experiments run in triplicate. Variation was generally 5–10%.

^b Cancer cells kindly supplied by State Key Laboratory of Pharmaceutical Biotechnology, Nanjing University.

^c Errors were in the range of 5–10% of the reported values, from three different assays.

^d Human recombinant enzymes, by the esterase assay (4-nitrophenylacetate as substrate).

2.2.4. Analysis of apoptosis by Annexin V-PE fluorescence-activated cell sorting (FACS)

To test whether the inhibition of cell growth of A549 was related to cell apoptosis, A549 cell apoptosis induced by compound **5d** was determined using flow cytometry. The uptake of Annexin V-PE was significantly increased, and the uptake of normal cells was significantly decreased in a time-dependent manner. Finally the percentage of early apoptotic cells was markedly elevated in a density-dependent manner from 6.28 to 19.6% at 48 h (Fig. 4).

2.3. Computational

2.3.1. Molecular modeling

To gain better understanding on the potency of the 18 compounds and guide further SAR studies, we proceeded to examine the interaction of these compounds with hCA II by molecular docking, which was performed by simulation of the 18 compounds into the ATP binding site in hCA II. The protein structure of the hCA II was downloaded from the PDB (3N4B.pdb) [28], then pre-processed using the Schrodinger Protein Preparation Guide. Also hydrogens were added to the structure, while H-bonds within the protein were optimized, and the protein was minimized to a rmsd of 0.3 Å. A 9.9 Å sphere of water molecules was added around the ligand and a short (3 ps) dynamics run was carried out, followed by several cycles of minimization using Quanta/CHARM. The entire protein–ligand–water complex was allowed to move during calculations [29].

The predicted binding interaction energy was used as the criterion for ranking. The estimated interaction energy of other synthesized compounds was ranging from –54.42 to –37.0 kcal/mol. The selected pose of **5a**, **5c** and **5d** had an estimated binding free energy of –39.4 kcal/mol, –43.5 kcal/mol, –47.6 kcal/mol, respectively. The binding model of compounds **5a**, **5c**, **5d** and hCA II was depicted in Fig. 5. The amino acid residues which had interaction with hCA II were labeled. In the binding mode, compound **5a** was nicely bound to the ATP binding site of hCA II hydrophobic interaction and the binding was stabilized by three hydrogen bonds. The hydrogens of Asn67 and Thr200 formed three hydrogen bonds interaction with nitrogen atom of C=N bonds of compound **5a** (angle N HD22 = 148.8°, distance = 2.30 Å), nitrogen atom of amino of compound **5a** (angle N H–N = 116.4°, distance = 2.46 Å) and hydrogen atom of amino of compound **5a** (angle H H–N = 133.8°, distance = 2.23 Å) each other. Besides, the hydrogen of Thr199, Gln92 and Trp5 formed three hydrogen bonds interaction with nitrogen atom of amino of compound **5c** (angle N H–N = 133.9°, distance = 2.10 Å), oxygen atom of sulfonyl of compound **5c** (angle

O HE21 = 135.7°, distance = 1.92 Å), and oxygen atom of carbonyl of compound **5c** (angle H H–N = 153.0°, distance = 2.23 Å) each other. And compound **5d** was also nicely bound to the ATP binding site of hCA II hydrophobic interaction and the binding was stabilized by two hydrogen bonds, and a π -cation interaction. The oxygen of the sulfonyl formed two hydrogen bonds with the backbone NH of Asn67 (angle O···H–N = 129.0°, distance = 2.17 Å), Gln92 (angle N–H···O = 137.7°, distance = 2.11 Å), respectively. In addition, a benzene ring formed one π - π interactions with Val135. This molecular docking result, along with the biological assay data, suggested that compounds **5a**, **5c** and **5d** were potential inhibitors of CA.

2.3.2. 3D-QSAR model [30]

In order to acquire a systematic SAR profile on sulfonamides containing coumarin moieties as antitumor agents and to explore the more powerful and selective dual hCA II and IX inhibitors, 3D-QSAR model was built to choose activity conformation of the designed molecular and reasonably evaluated the designed molecules by using the corresponding pIC₅₀ values which were converted from the obtained IC₅₀ (μM) values of hCA II inhibition and performed by built-in QSAR software of DS 3.5 (Discovery Studio 3.5, Accelrys, Co. Ltd). The way of this transformation was derived from an online calculator developed from an Indian medicinal chemistry lab (<http://www.sanjeevslab.org/tools-IC50.html>). The training and test set was divided by the random diverse molecules method of DS 3.5, in which the test set accounts for 83% while the training set was set to 17%. The training set composes 15 agents and 3 agents were consisted of the relative test set. The success of this model depended on docking study and the reliability of previous study about activities data.

In default situation, the alignment conformation of each molecule that possessed the lowest CDOCKER_INTERACTION_ENERGY among the eighteen docked poses. The 3D-QSAR model generated from DS 3.5, defined the critical regions (steric or electrostatic) affecting the binding affinity. It was a PLS model set up 400 independent variables (conventional R² = 0.861). The graphical relationship of observed and predicted values had been illustrated in Fig. 6a, in which the plot of the observed IC₅₀ versus the predicted values showed that this model could be used in prediction of activity for sulfonamides containing coumarin moieties.

A contour plot of the electrostatic field region favorable (in blue) or unfavorable (red) for anticancer activity based on hCA II protein target were shown in Fig. 6b while the energy grids corresponding to the favorable (in green) or unfavorable (yellow) steric effects for the hCA II affinity were shown in Fig. 6c. It was widely acceptable that a better inhibitor based on the 3D-QSAR model should have strong Van der Waals attraction in the green areas and a polar group in the blue electrostatic potential areas (which were dominant close to the skeleton). As shown in these two pictures, this promising model would provide a guideline to design and optimize more effective hCA II inhibitors based on the sulfonamides containing coumarin moieties and pave the way for us to further study in future.

Table 2

The median cytotoxic concentration (CC₅₀) data of tested compounds.

Compounds	5a	5c	5e	5g	5j	5l	5m	5g	5r
CC ₅₀ , μmol ^a	0.58	0.62	0.42	0.58	0.73	0.36	1.2	0.84	0.56

^a Minimum cytotoxic concentration required to cause a microscopically detectable alteration of normal cell morphology.

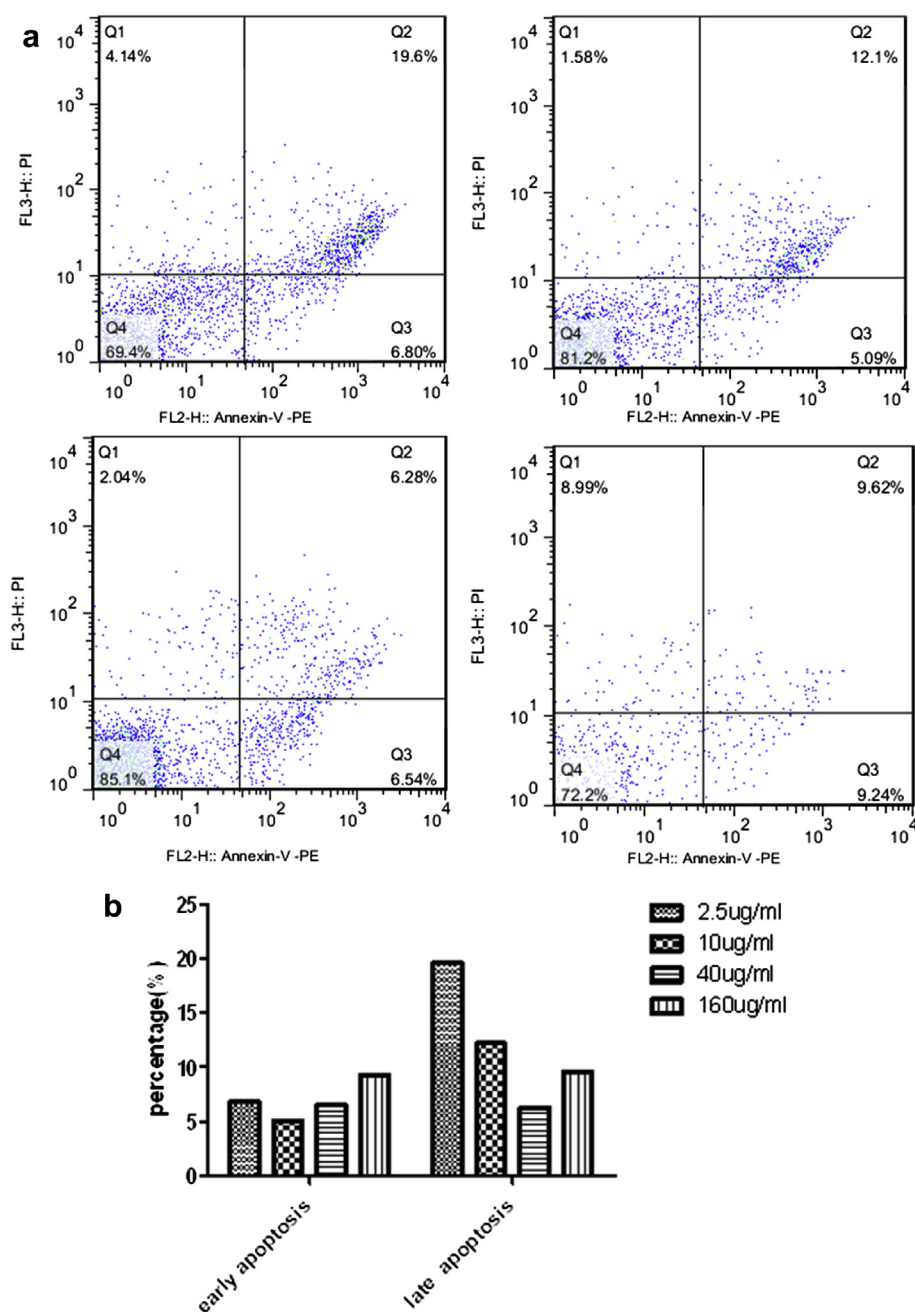


Fig. 4. Compound **5d** induced apoptosis in A549 cells with the density of 2.5, 10, 40, 160 µg/mL. A549 cells were treated with for 48 h. Values represent the mean, $n = 3$. $P < 0.05$ versus control. The percentage of cells in each part was indicated.

3. Conclusion

In summary, CA is an emerging target for the development of novel antitumor chemotherapeutics. We had designed and synthesized novel series of sulfonamides containing coumarin moieties which had been tested for their inhibitory activities against B16-F10 and MCF-7. These compounds showed a very interesting profile for the inhibition of hCAs II (cytosolic, off-target isoform) and hCAs IX (transmembrane, tumor-associated enzyme). Most of them exhibited CA inhibitory activities and almost no toxicity toward morphological. Docking simulation was performed to get the probable binding models and poses. Finally, QSAR models were built with previous activity data and

binding conformations to begin our work in this paper as well as to provide a reliable tool for reasonable design of CA inhibitors in future. The results indicate that sulfonamides containing coumarin moieties which acted as potent antibacterial activity and as such have the potential to be novel and potent antitumor agents. Given the unforeseen structural differences within the active site of some pathogenic enzymes, the key to discovering inhibitors with broad-spectrum antitumor activity lies in a detailed understanding of the CA active sites. Further studies on the CA inhibition ability of this compound, new structural data were guiding further modifications of the current series with the hopes of improving both enzymatic inhibition and physical properties.

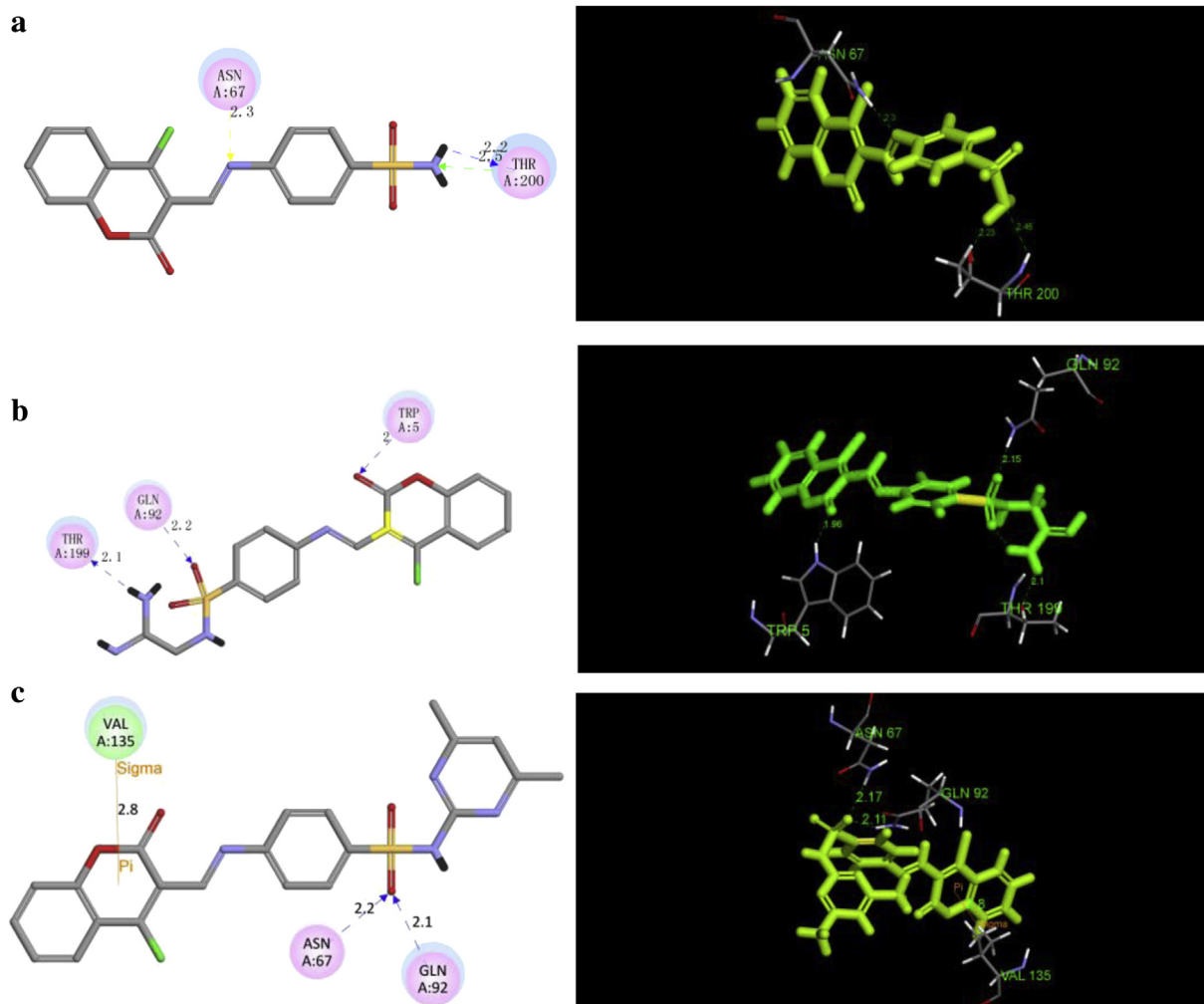


Fig. 5. Docking of compound **5a**, **5c** and **5d** in the ATP binding site of hCA II: (a) Left: 2D model of the interaction between compound **5a**, **5c**, **5d** and the ATP binding site. Right: 3D model of the interaction between compound **5a**, **5c**, **5d** and the ATP binding site, respectively.

4. Experiments

4.1. Materials and measurements

All chemicals used were purchased from Aldrich (USA). All reagents used in current study were of analytical grade. Thin layer chromatography (TLC) was performed on silica gel plates with fluorescent indicator. All analytical samples were homogeneous on TLC in at least two different solvent systems. Melting points (uncorrected) were determined on a X-4 MP apparatus (Taike Corp, Beijing, China). All the ^1H NMR spectra were recorded on a Bruker DPX 300 model Spectrometer in $\text{DMSO}-d_6$ and chemical shifts (δ) were reported as parts per million (ppm). ESI-MS spectra were recorded on a Mariner System 5304 Mass spectrometer. Elemental analyses were performed on a CHN-O-Rapid instrument and were within $\pm 0.4\%$ of the theoretical values.

4.2. General procedure for the synthesis of compounds **4a–4c**

Phosphorus oxychloride (10 mL) was added dropwise to a solution of dimethylformamide (DMF, 20 mL) keeping the temperature below $5\text{ }^\circ\text{C}$. Solution of different substituted 4-hydroxy-

2H-chromen-2-one (14.6 mmol) in DMF (10 mL) was then gradually added to the mixture with constant stirring and maintaining the temperature of the reaction mixture below $5\text{ }^\circ\text{C}$. The reaction mixture was then allowed to stand at room temperature for 2 h and then heated on a steam bath for 1 h. The reactions were monitored by thin layer chromatography (TLC). After cooling, the reaction mixture was poured onto crushed ice and neutralized with sodium carbonate. A solid product was immediately formed which was filtered, washed with water. And the crude products were purified by recrystallization with ethanol, ethyl acetate and petroleum ether (1:1:4) washed by ice-water (25 mL) for three times and dried to give a pure yellow solid product.

4.2.1. 4-Chloro-2-oxo-2H-chromene-3-carbaldehyde (**4a**) [31]

Yellow solid, yield 80%, m.p. $118\text{--}120\text{ }^\circ\text{C}$; ^1H NMR ($\text{DMSO}-d_6$, 300 MHz) δ : 10.35 (s, 1H, COH), 8.44–8.25 (m, 2H, ArH).

4.2.2. 4-Chloro-6-methyl-2-oxo-2H-chromene-3-carbaldehyde (**4b**) [32]

Yellow solid, yield 70%, m.p. $126\text{--}128\text{ }^\circ\text{C}$; ^1H NMR ($\text{DMSO}-d_6$, 300 MHz) δ : 10.35 (s, 1H, COH), 8.44–8.25 (m, 2H, ArH), 1.35 (s, 3H, CH_3).

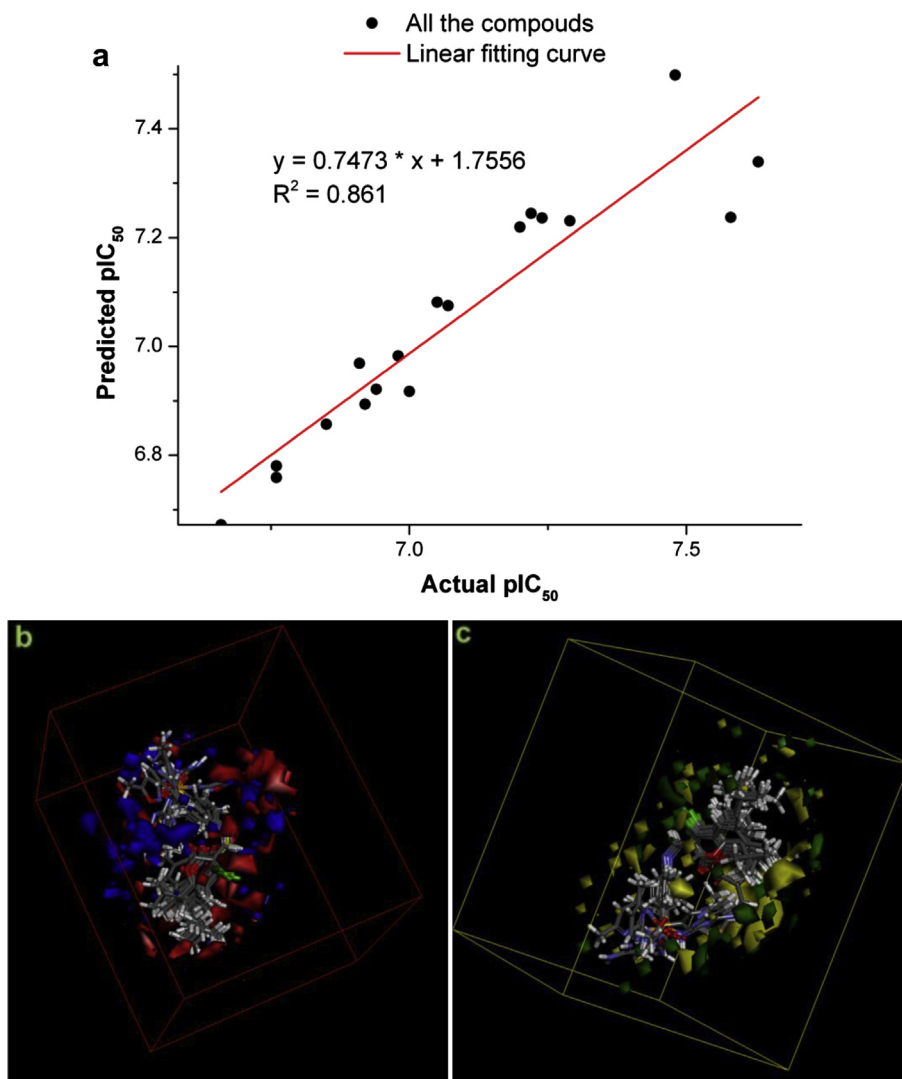


Fig. 6. (a) Using linear fitting curve to compare the predicted pIC_{50} value with that of experiment. (b) Isosurface of the 3D-QSAR model coefficients on electrostatic potential grids. The blue triangle mesh represents positive electrostatic potential and the red area represents negative electrostatic potential. (c) Isosurface of the 3D-QSAR model coefficients on Van der Waals grids. The green triangle mesh representation indicates positive coefficients; the yellow triangle mesh indicates negative coefficients. (For interpretation of the references to color in this figure legend, the reader is referred to the web version of this article.)

4.2.3. 6, 8-Ditertbutyl-4-chloro-2-oxo-2H-chromene-3-carbaldehyde (**4c**)

Yellow solid, yield 73%, m.p. 134–136 °C; 1H NMR (DMSO- d_6 , 300 MHz) δ : 10.35 (s, 1H, COH), 8.44–8.25 (m, 2H, ArH), 1.54 (s, 9H, C(CH $_3$) $_3$), 1.42 (s, 9H, C(CH $_3$) $_3$).

4.3. General procedure for the synthesis of compounds **5a–5r**

To a solution of compounds **4a–4c** (7.6 mmol) in ethanol (15 mL) was added different substituted sulfonamide (7.6 mmol) and acetic acid (0.5 mL). The mixture was heated at room temperature for 3 h. A solid product was immediately formed which was filtered, washed with water. And the crude products were purified by recrystallization with ethanol, ethyl acetate and acetone (1:1:0.5) washed by ice-water (25 mL) for three times and dried to give a yellow solid product **5a–5r**.

4.3.1. 4-((4-Chloro-2-oxo-2H-chromen-3-yl) methyleneamino) benzenesulfonamide (**5a**)

Yellow crystals, yield 79%, m.p. 271–273 °C; 1H NMR (DMSO- d_6 , 300 MHz) δ : 11.78 (s, 1H, SO $_2$ NH), 10.05 (s, 1H, CH), 7.89–7.07 (m,

8H, ArH), 3.80 (s, 2H, NH). ESI-MS: 363.61 [M + H] $^+$. Anal. Calcd for C $_{16}$ H $_{11}$ ClN $_2$ O $_4$ S: C, 52.97; H, 3.06; Cl, 9.77; N, 7.72; O, 17.64; S, 8.84; Found: C, 52.93; H, 3.07; Cl, 9.79; N, 7.71; O, 17.65; S, 8.85.

4.3.2. 4-((4-Chloro-2-oxo-2H-chromen-3-yl) methyleneamino)-N-(thiazol-2-yl) benzenesulfonamide (**5b**)

Yellow crystals, yield 73%, m.p. 276–278 °C; 1H NMR (DMSO- d_6 , 300 MHz) δ : 11.68 (s, 1H, SO $_2$ NH), 9.61 (s, 1H, –CH), 8.89–7.69 (m, 8H, ArH), 7.30 (s, $J = 2.7$ Hz, 1H, CH), 6.89 (s, $J = 2.7$ Hz, 1H, –CH), 6.90 (s, 1H, NH). ESI-MS: 446.811 [M + H] $^+$. Anal. Calcd for C $_{19}$ H $_{12}$ ClN $_3$ O $_4$ S $_2$: C, 51.18; H, 2.71; Cl, 7.95; N, 9.42; O, 14.35; S, 14.38; Found: C, 51.10; H, 2.73; Cl, 7.97; N, 9.43; O, 14.36; S, 14.40.

4.3.3. N-Carbamimidoyl-4-((4-chloro-2-oxo-2H-chromen-3-yl) methyleneamino) benzenesulfonamide (**5c**)

Orange crystals, yield 66%, m.p. 261–262 °C; 1H NMR (DMSO- d_6 , 300 MHz) δ : 11.70 (s, 1H, SO $_2$ NH), 10.01 (s, 1H, CH), 7.82–7.06 (m, 8H, ArH), 6.76 (s, 4H, NH). ESI-MS: 405.30 [M + H] $^+$. Anal. Calcd for C $_{17}$ H $_{13}$ ClN $_4$ O $_4$ S: C, 50.44; H, 3.24; Cl, 8.76; N, 13.84; O, 15.81; S, 7.92; Found: 50.40; H, 3.26; Cl, 8.78; N, 13.81; O, 15.82; S, 7.95.

4.3.4. 4-((4-Chloro-2-oxo-2H-chromen-3-yl) methyleneamino)-N-(4, 6-dimethyl-pyrimidin-2-yl) benzenesulfonamide (**5d**)

Yellow crystals, yield 62%, m.p. 245–247 °C; ¹H NMR (DMSO-*d*₆, 300 MHz) δ: 11.65 (s, 1H, SO₂NH), 9.63 (s, 1H, CH), 9.01 (s, 1H, CH), 8.94–7.33 (m, 8H, ArH), 2.24 (s, 6H, CH₃). ESI-MS: 469.90 [M + H]⁺. Anal. Calcd for C₂₂H₁₇ClN₄O₄S: C, 56.35; H, 3.65; Cl, 7.56; N, 11.95; O, 13.65; S, 6.84; Found: C, 56.30; H, 3.63; Cl, 7.59; N, 11.97; O, 13.66; S, 6.85.

4.3.5. 4-((4-Chloro-2-oxo-2H-chromen-3-yl) methyleneamino)-N-(5-methylisoxazol-3-yl) benzenesulfonamide (**5e**)

Yellow crystals, yield 63%, m.p. 245–247 °C; ¹H NMR (DMSO-*d*₆, 300 MHz) δ: 11.73 (s, 1H, SO₂NH), 9.61 (s, 1H, CH), 8.96–7.44 (m, 8H, ArH), 6.2 (s, *J* = 0.8 Hz, 1H, CH), 2.29 (s, 6H, CH₃). ESI-MS: 445.56 [M + H]⁺. Anal. Calcd for C₂₀H₁₄ClN₃O₅S: C, 54.12; H, 3.18; Cl, 7.99; N, 9.47; O, 18.02; S, 7.22; Found: C, 54.11; H, 3.19; Cl, 7.82; N, 9.45; O, 18.03; S, 7.20.

4.3.6. 4-((4-Chloro-2-oxo-2H-chromen-3-yl) methyleneamino)-N-(4-methylpyrimidin-2-yl) benzenesulfonamide (**5f**)

Yellow crystals, yield 88%, m.p. 245–247 °C; ¹H NMR (DMSO-*d*₆, 300 MHz) δ: 11.68 (s, 1H, SO₂NH), 9.64 (s, 1H, CH), 9.04 (s, *J* = 5.2 Hz, 1H, CH), 8.68–7.47 (m, 8H, ArH), 6.86 (d, *J* = 5.2 Hz, 1H, –CH), 2.31 (s, 3H, CH₃). ESI-MS: 455.9 [M + H]⁺. Anal. Calcd for C₂₁H₁₅ClN₄O₄S: C, 55.45; H, 3.32; Cl, 7.79; N, 12.32; O, 14.07; S, 7.05; Found: C, 55.38; H, 3.31; Cl, 7.80; N, 12.36; O, 14.09; S, 7.06.

4.3.7. 4-((6, 8-Di-tert-butyl-4-chloro-2-oxo-2H-chromen-3-yl) methyleneamino) benzenesulfonamide (**5g**)

Yellow crystals, yield 45%, m.p. >300 °C; ¹H NMR (DMSO-*d*₆, 300 MHz) δ: 9.61 (s, 1H, CH), 7.64 (s, 2H, NH), 8.81–7.66 (m, 6H, ArH), 1.52 (s, 9H, C(CH₃)₃), 1.40 (s, 9H, C(CH₃)₃). ESI-MS: 476.2 [M + H]⁺. Anal. Calcd for C₂₄H₂₇ClN₂O₄S: C, 60.69; H, 5.73; Cl, 7.46; N, 5.90; O, 13.47; S, 6.75; Found: C, 60.65; H, 5.75; Cl, 7.45; N, 5.92; O, 13.51; S, 7.08.

4.3.8. 4-((6, 8-Di-tert-butyl-4-chloro-2-oxo-2H-chromen-3-yl) methyleneamino)-N-(thiazol-2-yl) benzenesulfonamide (**5h**)

Yellow crystals, yield 88%, m.p. >300 °C; ¹H NMR (DMSO-*d*₆, 300 MHz) δ: 11.74 (s, 1H, SO₂NH), 9.61 (s, 1H, –CH), 8.86–7.65 (m, 6H, ArH), 7.28 (s, *J* = 2.7 Hz, 1H, CH), 6.88 (s, *J* = 2.7 Hz, 1H, CH), 6.90 (s, 1H, NH), 1.50 (s, 9H, C(CH₃)₃), 1.39 (s, 9H, C(CH₃)₃). ESI-MS: 559.30 [M + H]⁺. Anal. Calcd for C₂₇H₂₈ClN₃O₄S₂: C, 58.10; H, 5.06; Cl, 6.35; N, 7.53; O, 11.47; S, 11.49; Found: C, 58.05; H, 5.05; Cl, 6.34; N, 7.57; O, 11.49; S, 11.50.

4.3.9. N-Carbamimidoyl-4-((6,8-di-tert-butyl-4-chloro-2-oxo-2H-chromen-3-yl) methyleneamino) benzenesulfonamide (**5i**)

Light yellow crystals, yield 70%, m.p. 286–288 °C; ¹H NMR (DMSO-*d*₆, 300 MHz) δ: 11.77 (s, 1H, SO₂NH), 9.52 (s, 1H, CH), 8.77–7.66 (m, 6H, ArH), 6.80 (s, 3H, NH), 1.51 (s, 9H, C(CH₃)₃), 1.39 (s, 9H, C(CH₃)₃). ESI-MS: 518.08 [M + H]⁺. Anal. Calcd for C₂₅H₂₉ClN₄O₄S: C, 58.07; H, 5.65; Cl, 6.86; N, 10.84; O, 12.38; S, 6.20; Found: C, 58.13; H, 5.62; Cl, 6.83; N, 10.83; O, 12.36; S, 6.22.

4.3.10. 4-((6,8-Di-tert-butyl-4-chloro-2-oxo-2H-chromen-3-yl) methyleneamino)-N-(4, 6-dimethylpyrimidin-2-yl) benzenesulfonamide (**5j**)

Yellow crystals, yield 51%, m.p. 140–142 °C; ¹H NMR (DMSO-*d*₆, 300 MHz) δ: 11.76 (s, 1H, SO₂NH), 9.63 (s, 1H, CH), 9.01 (s, 1H, CH), 8.94–7.33 (m, 8H, ArH), 2.24 (s, 6H, CH₃). 1.51 (s, 9H, C(CH₃)₃), 1.39 (s, 9H, C(CH₃)₃). ESI-MS: 582.3 [M + H]⁺. Anal. Calcd for C₃₀H₃₃ClN₄O₄S: C, 62.00; H, 5.72; Cl, 6.10; N, 9.64; O, 11.01; S, 5.52; Found: C, 62.18; H, 5.68; Cl, 6.06; N, 9.60; O, 9.97; S, 5.50.

4.3.11. 4-((6,8-Di-tert-butyl-4-chloro-2-oxo-2H-chromen-3-yl) methyleneamino)-N-(5-methylisoxazol-3-yl) benzenesulfonamide (**5k**)

Light yellow crystals, yield 63%. m.p. 217–219 °C; ¹H NMR (DMSO-*d*₆, 300 MHz) δ: 11.68 (s, 1H, SO₂NH), 9.65 (s, 1H, –CH), 8.96–7.44 (m, 8H, ArH), 6.23 (s, *J* = 0.8 Hz, 1H, CH), 2.29 (s, 6H, CH₃). 1.53 (s, 9H, C(CH₃)₃), 1.41 (s, 9H, C(CH₃)₃). ESI-MS: 557.01 [M + H]⁺. Anal. Calcd for C₂₈H₃₀ClN₃O₅S: C, 60.48; H, 5.44; Cl, 6.38; N, 7.56; O, 14.39; S, 5.77; Found: C, 60.40; H, 5.45; Cl, 6.39; N, 7.58; O, 14.42; S, 5.78.

4.3.12. 4-((6,8-Di-tert-butyl-4-chloro-2-oxo-2H-chromen-3-yl) methyleneamino)-N-(4-methylpyrimidin-2-yl) benzenesulfonamide (**5l**)

Yellow crystals, yield 88%. m.p. 245–247 °C; ¹H NMR (DMSO-*d*₆, 300 MHz) δ: 11.66 (s, 1H, SO₂NH), 9.64 (s, 1H, CH), 9.04 (s, *J* = 5.2 Hz, 1H, CH), 8.68–7.47 (m, 8H, ArH), 6.86 (d, *J* = 5.2 Hz, 1H, CH), 2.31 (s, 3H, CH₃), 1.53 (s, 9H, C(CH₃)₃), 1.41 (s, 9H, C(CH₃)₃). ESI-MS: 568.40 [M + H]⁺. Anal. Calcd for C₂₉H₃₁ClN₄O₄S: C, 61.42; H, 5.51; Cl, 6.25; N, 9.88; O, 11.29; S, 5.65; Found: C, 61.49; H, 5.50; Cl, 6.23; N, 9.92; O, 11.30; S, 5.66.

4.3.13. 4-((4-Chloro-6-methyl-2-oxo-2H-chromen-3-yl) methyleneamino) benzene-sulfonamide (**5m**)

Yellow crystals, yield 57%. m.p. >300 °C; ¹H NMR (DMSO-*d*₆, 300 MHz) δ: 11.71 (s, 1H, SO₂NH), 9.54 (s, 1H, CH), 8.80–7.29 (m, 7H, ArH), 2.45 (s, 3H, CH₃). ESI-MS: 377.59 [M + H]⁺. Anal. Calcd for C₁₇H₁₃ClN₂O₄S: C, 54.19; H, 3.48; Cl, 9.41; N, 7.43; O, 16.98; S, 8.51; Found: C, 54.10; H, 3.50; Cl, 9.44; N, 7.42; O, 16.99; S, 8.52.

4.3.14. 4-((4-Chloro-6-methyl-2-oxo-2H-chromen-3-yl) methyleneamino)-N-(thiazol-2-yl) benzenesulfonamide (**5n**)

Yellow crystals, yield 58%. m.p. 225–227 °C; ¹H NMR (DMSO-*d*₆, 300 MHz) δ: 11.62 (s, 1H, SO₂NH), 9.56 (s, 1H, –CH), 8.86–7.45 (m, 6H, ArH), 7.32 (s, *J* = 5.0 Hz, 1H, –CH), 7.29 (s, 1H, ArH), 6.90 (s, *J* = 5.0 Hz, 1H, –CH), 6.90 (s, 1H, NH), 2.43 (s, 3H, CH₃). ESI-MS: 460.68 [M + H]⁺. Anal. Calcd for C₂₀H₁₄ClN₃O₄S₂: C, 52.23; H, 3.07; Cl, 7.71; N, 9.14; O, 13.91; S, 13.94; Found: C, 52.18; H, 3.08; Cl, 7.70; N, 9.13; O, 13.94; S, 13.98.

4.3.15. N-Carbamimidoyl-4-((4-chloro-6-methyl-2-oxo-2H-chromen-3-yl) methylene-amino) benzenesulfonamide (**5o**)

Light yellow crystals, yield 50%. m.p. 250–252 °C; ¹H NMR (DMSO-*d*₆, 300 MHz) δ: 11.59 (s, 1H, SO₂NH), 9.52 (s, 1H, CH), 7.83–7.23 (m, 6H, ArH), 6.77 (s, 3H, NH), 2.39 (s, 3H, CH₃). ESI-MS: 419.91 [M + H]⁺. Anal. Calcd for C₁₈H₁₅ClN₄O₄S: C, 51.62; H, 3.61; Cl, 8.46; N, 13.38; O, 15.28; S, 7.66; Found: C, 51.56; H, 3.64; Cl, 8.43; N, 13.42; O, 15.31; S, 7.65.

4.3.16. 4-((4-Chloro-6-methyl-2-oxo-2H-chromen-3-yl) methyleneamino)-N-(4,6-dimethylpyrimidin-2-yl) benzenesulfonamide (**5p**)

Orange crystals, yield 51%. m.p. 170–172 °C; ¹H NMR (DMSO-*d*₆, 300 MHz) δ: 11.59 (s, 1H, SO₂NH), 9.58 (s, 1H, CH), 8.98–7.28 (m, 8H, ArH), 6.70 (s, 1H, CH), 2.42 (s, 3H, CH₃), 2.23 (s, 6H, CH₃). ESI-MS: 483.81 [M + H]⁺. Anal. Calcd for C₂₃H₁₉ClN₄O₄S: C, 57.20; H, 3.97; Cl, 7.34; N, 11.60; O, 13.25; S, 6.64; Found: C, 57.10; H, 3.98; Cl, 7.36; N, 11.62; O, 13.27; S, 6.65.

4.3.17. 4-((4-Chloro-6-methyl-2-oxo-2H-chromen-3-yl) methyleneamino)-N-(5-methylisoxazol-3-yl) benzenesulfonamide (**5q**)

Orange crystals, yield 55%. m.p. 240–242 °C; ¹H NMR (DMSO-*d*₆, 300 MHz) δ: 11.78 (s, 1H, SO₂NH), 9.51 (s, 1H, CH), 8.88–7.33 (m, 7H, ArH), 6.23 (s, *J* = 0.9 Hz, 1H, CH), 2.36 (s, 3H, CH₃). 2.22 (s, 3H, CH₃). ESI-MS: 458.92 [M + H]⁺. Anal. Calcd for C₂₁H₁₆ClN₃O₅S: C, 55.08; H, 3.52; Cl, 7.74; N, 9.18; O, 17.47; S, 7.00; Found: C, 55.00; H, 3.54; Cl, 7.76; N, 9.22; O, 17.50; S, 6.99.

4.3.18. 4-((4-Chloro-6-methyl-2-oxo-2H-chromen-3-yl)methyleneamino)-N-(4-methylpyrimidin-2-yl) benzenesulfonamide (5r)

Yellow crystals, yield 74%. m.p. 273–275 °C; ¹H NMR (DMSO-*d*₆, 300 MHz) δ: 11.76 (s, 1H, SO₂NH), 9.64 (s, 1H, CH), 9.97 (d, *J* = 2.0 Hz, 1H, CH), 8.42–7.32 (m, 7H, ArH), 6.78 (d, *J* = 5.2 Hz, 1H, –CH), 2.44 (s, 3H, CH₃), 2.27 (s, 3H, CH₃). ESI-MS: 469.83 [M + H]⁺. Anal. Calcd for C₂₂H₁₇ClN₄O₄S: C, 56.35; H, 3.65; Cl, 7.56; N, 11.95; O, 13.65; S, 6.84; Found: C, 56.30; H, 3.63; Cl, 7.58; N, 11.97; O, 13.67; S, 6.85.

4.4. CA inhibition assay

An Applied Photophysics stopped-flow instrument has been used for assaying the CA-catalyzed CO₂ hydration activity [33]. Phenol red (at a concentration of 0.2 mM) has been used as indicator, working at the absorbance maximum of 557 nm, with 10 mM Hepes (pH = 7.5) as buffer, 0.1 M Na₂SO₄ (for maintaining constant the ionic strength), at 25 °C, following the CA-catalyzed CO₂ hydration reaction for a period of 10–100 s (the uncatalyzed reaction needs around 60–100 s in the assay conditions, whereas the catalyzed ones are of around 6–10 s). The CO₂ concentrations ranged from 1.7 to 17 mM for the determination of kinetic parameters. For each inhibitor, tested in the concentration range between 0.01 nM and 100 μM, at least six traces of the initial 5–10% of the reaction have been used for determining the initial velocity. The uncatalyzed rates were determined in the same manner and subtracted from the total observed rates. Stock solutions of inhibitor (1 mM) were prepared in distilled–deionized water with 10–20% (v/v) DMSO (which is not inhibitory at these concentrations), and dilutions up to 0.01 nM were done thereafter with distilled–deionized water. Inhibitor and enzyme solutions were preincubated together for 15 min at room temperature prior to assay, in order to allow for the formation of the E–I complex. The inhibition constants were obtained by nonlinear least-squares methods using PRISM₃. The curve-fitting algorithm allowed us to obtain the IC₅₀ values, working at the lowest concentration of substrate of 1.7 mM, from which *K_i* values were calculated by using the Cheng–Prusoff equation. The catalytic activity (in the absence of inhibitors) of these enzymes was calculated from Lineweaver–Burk plots, as reported earlier, and represents the mean from at least three different determinations. 38–42 Enzyme concentrations in the assay system were 7.3 nM for hCA II, and 8.5 nM for hCA IX. Enzymes used here were recombinant ones, prepared and purified as described earlier [34].

4.5. Cell proliferation assay

CCK-8 is much more convenient and helpful than MTT for analyzing cell proliferation, because it can be reduced to soluble formazan by dehydrogenase in mitochondria and has little toxicity to cells. Cell proliferation was determined using CCK-8 dye (Beyotime Inst Biotech, China) according to manufacture's instructions. Briefly, 1–5 × 10³ cells per well were seeded in a 96-well plate, grown at 37 °C for 12 h. Subsequently, cells were treated with the target compounds at increasing concentrations in the presence of 10% FBS for 24 or 48 h. After 10 μL CCK-8 dye was added to each well, cells were incubated at 37 °C for 1–2 h and Plates were read in a Victor-V multilabel counter (Perkin–Elmer) using the default europium detection protocol. Percent inhibition or IC₅₀ values of compounds were calculated by comparison with DMSO-treated control wells.

4.6. Flow cytometry

Cells (1.3 × 10⁵ cells/mL) were cultured in the presence or not of novobiocin analogues at 200 μM. Nvb at the same concentration

served as reference inhibitor. After treatment for 48 and 72 h, cells were washed and fixed in PBS/ethanol (30/70). For cytofluorometric examination, cells (10⁴ cells/mL) were incubated for 30 min in PBS/Triton X100, 0.2%/EDTA 1 mM, and propidium iodide (PI) (50 μg/mL) in PBS supplemented by RNase (0.5 mg/mL). The number of cells in the different phases of the cell cycle was determined, and the percentage of apoptotic cells was quantified. Analyses were performed with a FACS Calibur (Becton Dickinson, Le Pont de Claix, France). Cell Quest software was used for data acquisition and analysis [35].

4.7. Experimental protocol of docking study

Molecular docking of compound **5a**, **5c** and **5d** into the three dimensional X-ray structure of human hCA II (PDB code: 3N4B) was carried out using the Discovery Studio (version 3.5) as implemented through the graphical user interface DS-CDOCKER protocol. The three-dimensional structures of the aforementioned compounds were constructed using Chem. 3D ultra 12.0 software [Chemical Structure Drawing Standard; Cambridge Soft corporation, USA (2010)], then they were energetically minimized by using MMFF94 with 5000 iterations and minimum RMS gradient of 0.10. The crystal structures of protein complex was retrieved from the RCSB Protein Data Bank (<http://www.rcsb.org/pdb/home/home.do>). All bound waters and ligands were eliminated from the protein and the polar hydrogen was added to the proteins. Molecular docking of all twenty compounds was then carried out using the Discovery Studio (version 3.5) as implemented through the graphical user interface CDOCKER protocol. CDOCKER is an implementation of a CHARMm based molecular docking tool using a rigid receptor.

4.8. 3D-QSAR

Ligand-based 3D-QSAR approach was performed by QSAR software of DS 3.5 (Discovery Studio 3.5, Accelrys, Co. Ltd). The training sets were composed of inhibitors with the corresponding pIC₅₀ values which were converted from the obtained IC₅₀ (μM), and test sets comprised compounds of data sets. All the definition of the descriptors can be seen in the “Help” of DS 3.5 software and they were calculated by QSAR protocol of DS 3.5. The alignment conformation of each molecule was the one with lowest interaction energy in the docked results of CDOCKER. The predictive ability of 3D-QSAR modeling can be evaluated based on the cross-validated correlation coefficient, which qualifies the predictive ability of the models. Scrambled test (Y scrambling) was performed to investigate the risk of chance correlations. The inhibitory potencies of compounds were randomly reordered for 30 times and subject to leave-one-out validation test, respectively. The models were also validated by test sets, in which the compounds are not included in the training sets. Usually, one can believe that the modeling is reliable, when the R² for test sets is larger than 0.6.

Acknowledgments

The work was financed by a grant (No. J1103512) from National Natural Science Foundation of China and a grant (No. CXLX12_0047) from Jiangsu Ordinary University Graduate Students Scientific Research Innovation Plan of China.

References

- [1] A. Cincinelli, T. Martellini, A. Innocenti, A. Scozzafava, C.T. Supuran, Purification and inhibition studies with anions and sulfonamides of an α-carbonic anhydrase from the Antarctic seal *Leptonychotes weddellii*, *Bioorg. Med. Chem.* 19 (2011) 1847–1851.

- [2] B.L. Wilkinson, L.F. Bornaghi, T.A. Houston, A. Innocenti, D. Vullo, C.T. Supuran, S.A. Poulsen, Carbonic anhydrase inhibitors: inhibition of isozymes I, II, and IX with triazole-linked *o*-glycosides of benzene sulfonamides, *J. Med. Chem.* 50 (2007) 1651–1657.
- [3] M. Lopez, L.F. Bornaghi, A. Innocenti, D. Vullo, S.A. Charman, C.T. Supuran, S.A. Poulsen, Sulfonamide linked neoglycoconjugates—a new class of inhibitors for cancer-associated carbonic anhydrases, *J. Med. Chem.* 53 (2010) 2913–2926.
- [4] M. Hilvo, L. Baranauskiene, A.M. Salzano, A. Scaloni, D. Matulis, A. Innocenti, A. Scozzafava, S.M. Monti, A. Di Fiore, G. De Simone, M. Lindfors, J. Janis, J. Valjakka, S. Pastorekova, J. Pastorek, M.S. Kulomaa, H.R. Nordlund, C.T. Supuran, S. Parkkila, Biochemical characterization of CA IX: one of the most active carbonic anhydrase isozymes, *J. Biol. Chem.* 283 (2008) 27799–27809.
- [5] J. Chiche, K. Ilc, J. Laferriere, E. Trotter, F. Dayan, N.M. Mazure, M.C. Brahimi-Horn, J. Pouyssegur, Hypoxia-inducible carbonic anhydrase IX and XII promote tumor cell growth by counteracting acidosis through the regulation of the intracellular pH, *Cancer Res.* 69 (2009) 358–368.
- [6] M.C. Brahimi-Horn, G. Bellot, J. Pouyssegur, Hypoxia and energetic tumour metabolism, *Curr. Opin. Genet. Dev.* 21 (2011) 67–72.
- [7] J.C. Morris, J. Chiche, C. Grellier, M. Lopez, L.F. Bornaghi, A. Maresca, C.T. Supuran, Jacques. Pouyssegur, S.A. Poulsen, *J. Med. Chem.* 54 (2011) 6905–6918.
- [8] P. Swietach, R. Vaughan-Jones, A. Harris, Regulation of tumor pH and the role of carbonic anhydrase 9, *Cancer Metastasis Rev.* 26 (2007) 299–310.
- [9] E. Svastova, A. Hulikova, M. Rafajova, M. Zatovicova, A. Gibaduli-nova, A. Casini, A. Cecchi, A. Scozzafava, C.T. Supuran, J. Pastorek, S. Pastorekova, Hypoxia activates the capacity of tumor-associated carbonic anhydrase IX to acidify extracellular pH, *FEBS Lett.* 577 (2004) 439–445.
- [10] F. Pacchiano, F. Carta, P.C. McDonald, Y.M. Lou, D. Vullo, A. Scozzafava, S. Dedhar, C.T. Supuran, Ureido-substituted benzenesulfonamides potently inhibit carbonic anhydrase IX and show inhibitory activity in a model of breast cancer metastasis, *J. Med. Chem.* 54 (2011) 1896–1902.
- [11] C.T. Supuran, F. Briganti, S. Tilli, W.R. Chegwidden, A. Scozzafava, Carbonic anhydrase inhibitors: sulfonamides as antitumor agents, *Bioorg. Med. Chem.* 9 (2001) 703–714.
- [12] (a) C.C. Wykoff, N.J. Beasley, P.H. Watson, K.J. Pastorek, J. Turner, A. Sibtain, G.D. Wilson, H. Turley, K.L. Talks, P.H. Maxwell, C.W. Pugh, P.J. Ratcliffe, A.L. Harris, Hypoxia-inducible regulation of tumor-associated carbonic anhydrases, *Cancer Res.* 60 (2000) 7075–7083;
(b) C.P.S. Potter, A.L. Harris, Diagnostics, prognostics and therapeutic implications of carbonic anhydrases in cancer, *Br. J. Cancer* 89 (2003) 2–7;
(c) R.K. Jain, Normalization of tumor vasculature: an emerging concept in antiangiogenic therapy, *Science* 307 (2005) 58–62.
- [13] W.A. Denny, Tumor-activated prodrugs. A new approach to cancer therapy, *Cancer Invest.* 22 (2004) 604–619.
- [14] J. Chiche, M. Brahimi-Horn, J. Pouyssegur, Tumor hypoxia induces a metabolic shift causing acidosis: a common feature in cancer, *J. Cell. Mol. Med.* 14 (2010) 771–794.
- [15] Y. Yoshino, N. Ueda, J. Nijima, H. Sugumi, Y. Kotake, N. Koyanagi, K. Yoshimatsu, M. Asada, T. Watanabe, T. Nagasu, K. Tsukahara, A. Iijima, K.J. Kitoh, *Med. Chem.* 35 (1992) 2496–2497.
- [16] A. Casini, A. Scozzafava, A. Mastrolorenzo, C.T. Supuran, Sulfonamides and sulfonylated derivatives as anticancer agents, *Curr. Cancer Drug Targets* 2 (2002) 55–75.
- [17] B. Shan, J.C. Medina, E. Santha, W.P. Frankmoelle, T.C. Chou, R.M. Learned, M.R. Narbut, D. Stott, P. Wu, J.C. Jaen, T. Rosen, P.B.M.W.M. Timmermans, H. Beckmann, Proc. Selective, covalent modification of β -tubulin residue Cys-239 by T138067, an antitumor agent with in vivo efficacy against multidrug-resistant tumors, *Natl. Acad. Sci. U. S. A.* 96 (1999) 5686–5691.
- [18] H. Tanaka, N. Ohshima, M. Ikenoya, K. Komori, F. Katoh, H. Hidaka, HMN-176, an active metabolite of the synthetic antitumor agent HMN-214, restores chemosensitivity to multidrug-resistant cells by targeting the transcription factor NF- κ B, *Cancer Res.* 63 (2003) 6942–6947.
- [19] C.T. Supuran, A. Scozzafava, Carbonic anhydrase inhibitors and their therapeutic potential, *Exp. Opin. Ther. Patents* 10 (2000) 575–600.
- [20] J. Drew, Drug discovery: a historical perspective, *Science* 287 (2000) 1960–1964.
- [21] R. Bashir, S. Ovais, S. Yaseen, H. Hamid, M.S. Alam, M. Samim, S. Singh, K. Javed, Synthesis of some new 1,3,5-trisubstituted pyrazolines bearing benzene sulfonamide as anticancer and anti-inflammatory agents, *Bioorg. Med. Chem.* 21 (2011) 4301–4305.
- [22] A. Maresca, C. Temperini, L. Pochet, B. Masereel, A. Scozzafava, C.T. Supuran, Deciphering the mechanism of carbonic anhydrase inhibition with coumarins and thiocoumarins, *J. Med. Chem.* 53 (2010) 335–344.
- [23] C.T. Supuran, A. Scozzafava, A. Casini, *Med. Res. Rev.* 23 (2003) 146–189.
- [24] A. Thiery, M. Ledecq, A. Cecchi, J.M. Dogne, J. Wouters, C.T. Supuran, B.J. Masereel, *Med. Chem.* 49 (2006) 2743–2749.
- [25] W.T. Gao, W.R. Hou, M.R. Zheng, *Chin. J. Org. Chem.* 28 (2008) 2011–2015.
- [26] R.G. Khalifah, The carbon dioxide hydration activity of carbonic anhydrase I. Stop-flow kinetic studies on the native human isoenzymes B and C, *J. Biol. Chem.* 246 (1971) 2561–2573.
- [27] (a) C.T. Supuran, Carbonic anhydrases: novel therapeutic applications for inhibitors and activators, *Nat. Rev. Drug Discov.* 7 (2008) 168–181;
(b) O. Ozsenoy, G. De Simone, C.T. Supuran, Drug design studies of the novel antitumor targets carbonic anhydrase IX and XII, *Curr. Med. Chem.* 17 (2010) 1516–1526;
(c) G. De Simone, C.T. Supuran, Carbonic anhydrase IX: biochemical and crystallographic characterization of a novel antitumor target, *Biochim. Biophys. Acta* 1804 (2010) 404–409;
(d) C.T. Supuran, Carbonic anhydrase inhibitors, *Bioorg. Med. Chem. Lett.* 20 (2010) 3467–3474.
- [28] F. Pacchiano, M. Aggarwal, B.S. Avvaru, A.H. Robbins, A. Scozzafava, R. McKenna, C.T. Supuran, Selective hydrophobic pocket binding observed within the carbonic anhydrase II active site accommodate different 4-substituted-ureido-benzenesulfonamides and correlate to inhibitor potency, *Chem. Commun. (Cambridge, U. K.)* 46 (2010) 8371–8373.
- [29] L.T. Webster, A. Gilman, T.W. Rall, A.S. Nies, P. Taylor, Drugs used in the chemotherapy of protozoal infections, in: *The Pharmacological Basis of the Rapeutics*, eighth ed., Pergamon Press, New York, 1990, pp. 999–1007.
- [30] W.J. Egan, K.J. Merz, J.J. Baldwin, Prediction of drug absorption using multivariate statistics, *J. Med. Chem.* 43 (2000) 3867–3877.
- [31] L. Dawara, R.V. Singh, Synthesis, spectroscopic characterization, antimicrobial, pesticidal and nematocidal activity of some nitrogen-oxygen and nitrogen-sulfur donor coumarins based ligands and their organotin(IV) complexes, *Appl. Organomet. Chem.* 25 (2011) 643–652.
- [32] A. Kasabe, G.V. Mohite, J. Vidhate, Synthesis, characterization and primary antimicrobial, antifungal activity evaluation of Schiff bases of 4-chloro- (3-substituted-phenylimino)-methyl-[2H]-chromene-2-one, *E-Journal Chem.* 7 (2010) 377–382.
- [33] R.G. Khalifah, The carbon dioxide hydration activity of carbonic anhydrase, *J. Biol. Chem.* 246 (1971) 2561–2573.
- [34] (a) J.Y. Winum, D. Vullo, A. Casini, J. L. Montero, A. Scozzafava, C.T. Supuran, Carbonic anhydrase inhibitors: inhibition of trans-membrane, tumor-associated isozyme IX, and cytosolic isozymes I and II with aliphatic sulfamates, *J. Med. Chem.* 46 (2003) 5471–5477;
(b) A. Cecchi, A. Hulikova, J. Pastorek, S. Pastorekova, A. Scozzafava, J.Y. Winum, J.L. Montero, C.T. Supuran, Carbonic anhydrase inhibitors. Sulfonamides inhibit isozyme IX mediated acidification of hypoxic tumors. Fluorescent sulfonamides design as probes of membrane-bound carbonic anhydrase isozymes involvement in tumorigenesis, *J. Med. Chem.* 48 (2005) 4834–4841;
(c) B.L. Wilkinson, L.F. Bornaghi, T.A. Houston, A. Innocenti, D. Vullo, C.T. Supuran, S.A. Poulsen, Carbonic anhydrase inhibitors: inhibition of isozymes I, II, and IX with triazole-linked *o*-glycosides of benzene sulfonamides, *J. Med. Chem.* 50 (2007) 1651–1657.
- [35] G.L. Bras, C. Radanyi, J.F. Peyrat, J.D. Brion, M. Alami, V. Marsaud, B. Stella, J.M. Renoir, New novobiocin analogues as antitumor agents in breast cancer cells and potential inhibitors of heat shock protein 90, *J. Med. Chem.* 50 (2007) 6189–6200.